This pdf file consists of figures containing photographs, and their captions, scanned from:

CENOZOIC TECTONICS OF THE CARIBBEAN:

STRUCTURAL AND STRATIGRAPHIC STUDIES IN JAMAICA AND HISPANIOLA

by

William Paul Mann

A Dissertation

Submitted to the State University of New York at Albany

in Partial Fulfillment of

the Requirements for the Degree of

Doctor of Philosophy

College of Science and Mathematics

Department of Geological Sciences

1983

INTRODUCTION

Orchids, Sierra de Neiba, Dominican Republic

PART 1

CENOZOIC TECTONICS OF THE CARIBBEAN

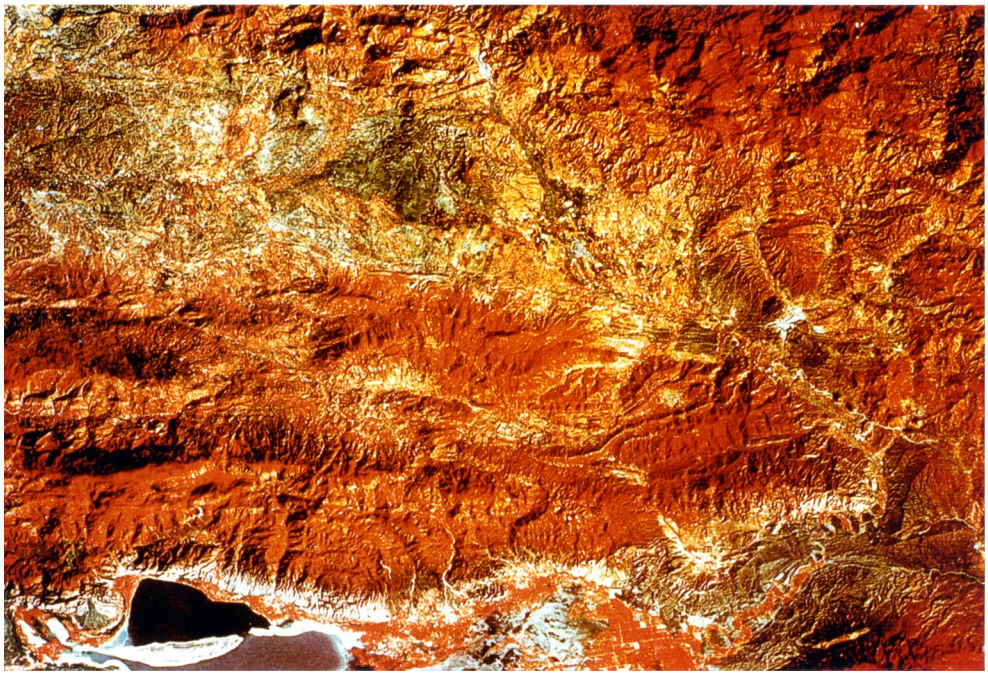

Enhanced color LANDSAT image of south-central Hispaniola: Enriquillo-Plantain Garden strike-slip Fault Zone obliquely crosses bottom of photograph; dark area at top center of photograph is area of Pleistocene basalt flows; recent volcanic cones are visible at right center of photograph (see Chapter 3 for interpretation).

Figure 6. Aerial view of the southwestern flank of Blue Mountains, Jamaica. Upthrusting along Neogene convergent left-lateral strike-slip fault in valley has produced the high topography of the Blue Mountains in the background (covered by clouds) and has exposed a major Paleocene unconformity separating Cretaceous arc rocks (upper right of photo) from a thin Paleocene linestone (Chepstow Limestone) and Paleocene clastic rocks (bottom and left of photo).

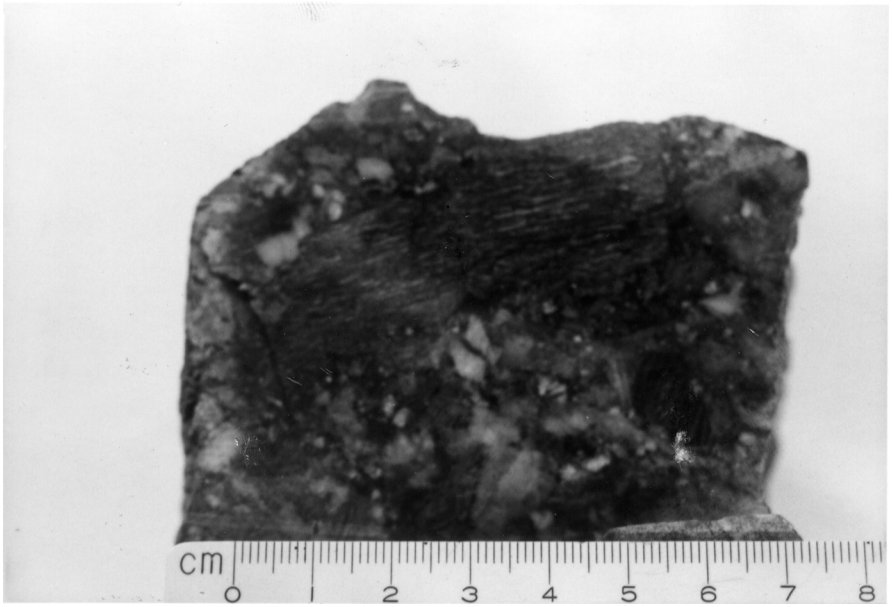

Figure 7. Polished face of a cobble of basal conglomerate found above unconformity in the southwestern Blue Mountains (area shown in Figure 6). Note poor sorting, angularity of clasts, and variable clast compositions that include quartz, schist, and volcanic rocks. Conglomerate indicates Paleogene uplift and deep level erosion of a late Cretaceous island arc.

Figure 8. Massive, nodular grey limestone of the Chepstow Formation, a thin reefal limestone lying about 10-15 m above the major Cretaceous-Tertiary unconformity and basal conglomerate in the southwestern Blue Mountains. Note shell fragments (pen is 14 cm long).

Figure 9. Major Cretaceous-Tertiary unconfomity suggested by geologic relationships in the Riviere Glace, Massif de la Macaya, southwestern Haiti: gently dipping limestone to right contains a planktonic foraminiferal and radiolarian fauna of medial to late Maestrichtian age (Macaya Fm.); float blocks on base slope to left of road are poorly sorted conglomerates shown in Figures 10 and 11 and contain resedimented late Cretaceous volcanics and deep water limestones and are overlain by Paleocene to lower Eocene shelf limestones. A major unconformity of earliest Tertiary age, although not exposed, appears to truncate the late Cretaceous limestone sequence.

Figure 10. Boulder of basal conglomerate on slope indicated in Figure 9. Three main clast components are: 1) late Cretaceous deep-water micrites (light pebbles) that contain distinctively keeled *Globotruncana sp.* of late Cretaceous age; 2) green porphyritic volcanics (dark pebbles); and 3) coral, rudist and shell debris (light pebbles). Pen to right is 14 cm long.

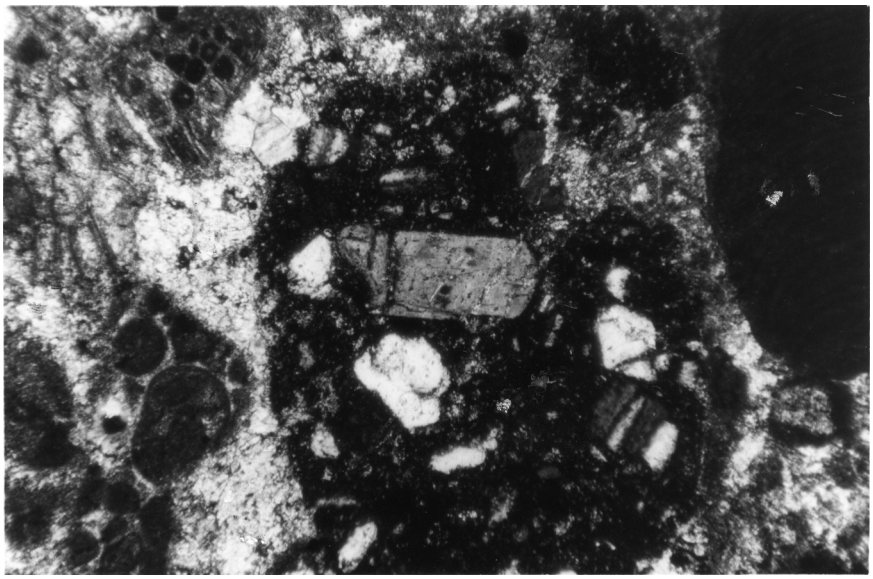

Figure 11. Photomicrograph of volcanic rock fragment in basal conglomerate shown in Figures 9 and 10 (crossed polars, 3.5x magnification). Note large laths of plagioclase with euhedral outline and well developed twinning set in finely crystalline matrix. Dark shape in right corner is *Archeolithothuramid* red coralline algae indicative of earliest Tertiary age (E. Robinson, pers. comm., 1983). Round shapes to left are assorted shell fragments. Note poikilotopic calcite cement in upper left that results from calcite crystallization between irregular distributed clasts.

Figure 12. Massive limestone blocks within volcaniclastic sandstone matrix along the Jacmel Road section, Massif de la Selle, southern Haiti. Lepinay et al. [1979] have tentatively identified Albian-Cenomanian faunas from the limestone blocks and a late Campanian or Maestrichtian fauna from the matrix. Note south-dipping faults cutting the outcrop which Lepinay et al. [1979] determined to be thrust faults active during the deposition of the limestone blocks within the volcaniclastic matrix.

Figure 13. Late Eocene terriginous turbidites with intercalated calcarenite exposed along the Bani-Azua highway, Sierra el Numero, Dominican Republic. Normal faults offsetting beds by one meter or less trend northeast and appear to be secondary faults related to Neogene east-west left-lateral strike-slip movements in Hispaniola.

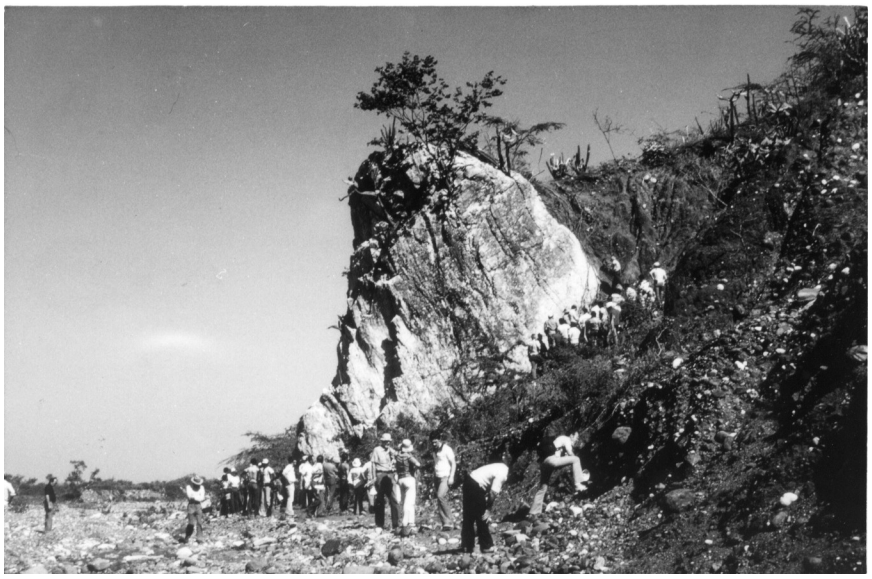

Figure 14. Angular olistolith of massive fine grained limestone in which Bourgois et al. [1979] identified medial Eocene larger foraminifera. Matrix is also of medial Eocene age and consists of terrigenous turbidites and occasional conglomerates with clasts of amphibolite, basalt, and gabbro. Note discordance between dip of well bedded conglomerate away from the viewer and bedding of massive limestone olistolith.

Figure 15. Well bedded, dense medial to late Eocene shelf-limestone (Neiba Fm.) unconformably overlying Paleogene arc rocks in the Sierra de Neiba, Dominican Republic. The limestone typically contains thin beds and nodules of brown chert.

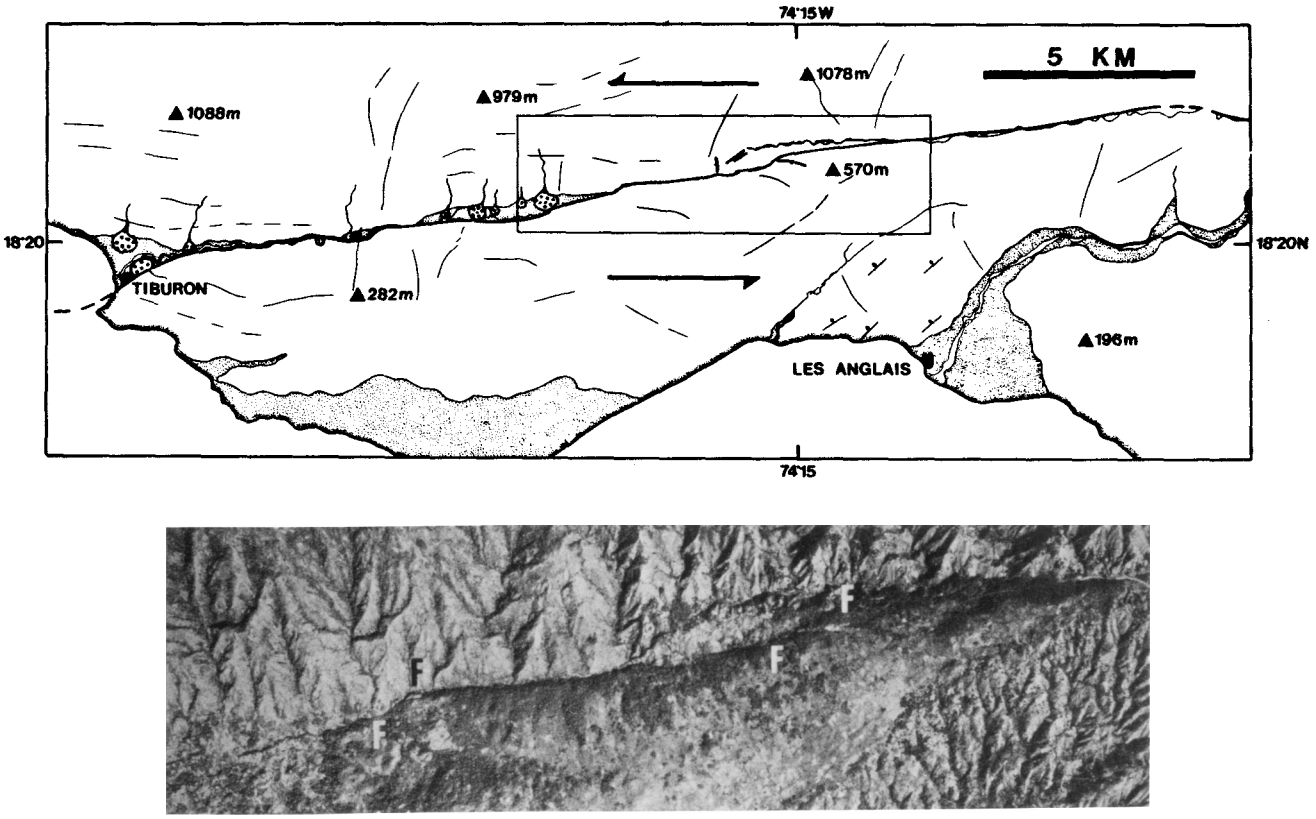

Fig 5. – Aerial photointerpretation of incipient pull-aparts forming at left-stepping releasing bends along the Enriquillo-Plaintain Garden Fault Zone in southwestern Haiti (see Fig. 4 for regional setting). Stippled areas represent alluvium; dotted areas are alluvial fans. Inset is aerial photograph showing details of "releasing bend" master fault geometry. Letter F marks approximate termination of dominant oblique fault segments at releasing bends. Overlapping of master fualts appears to be occurring at the easternmost bend.

PART 2

STRUCTURAL AND STRATIGRAPHIC STUDIES IN JAMAICA AND HISPANIOLA

Petroglyphs in Holocene algal tufa, Enriquillo Valley, Dominican Republic (see Chapter 6).

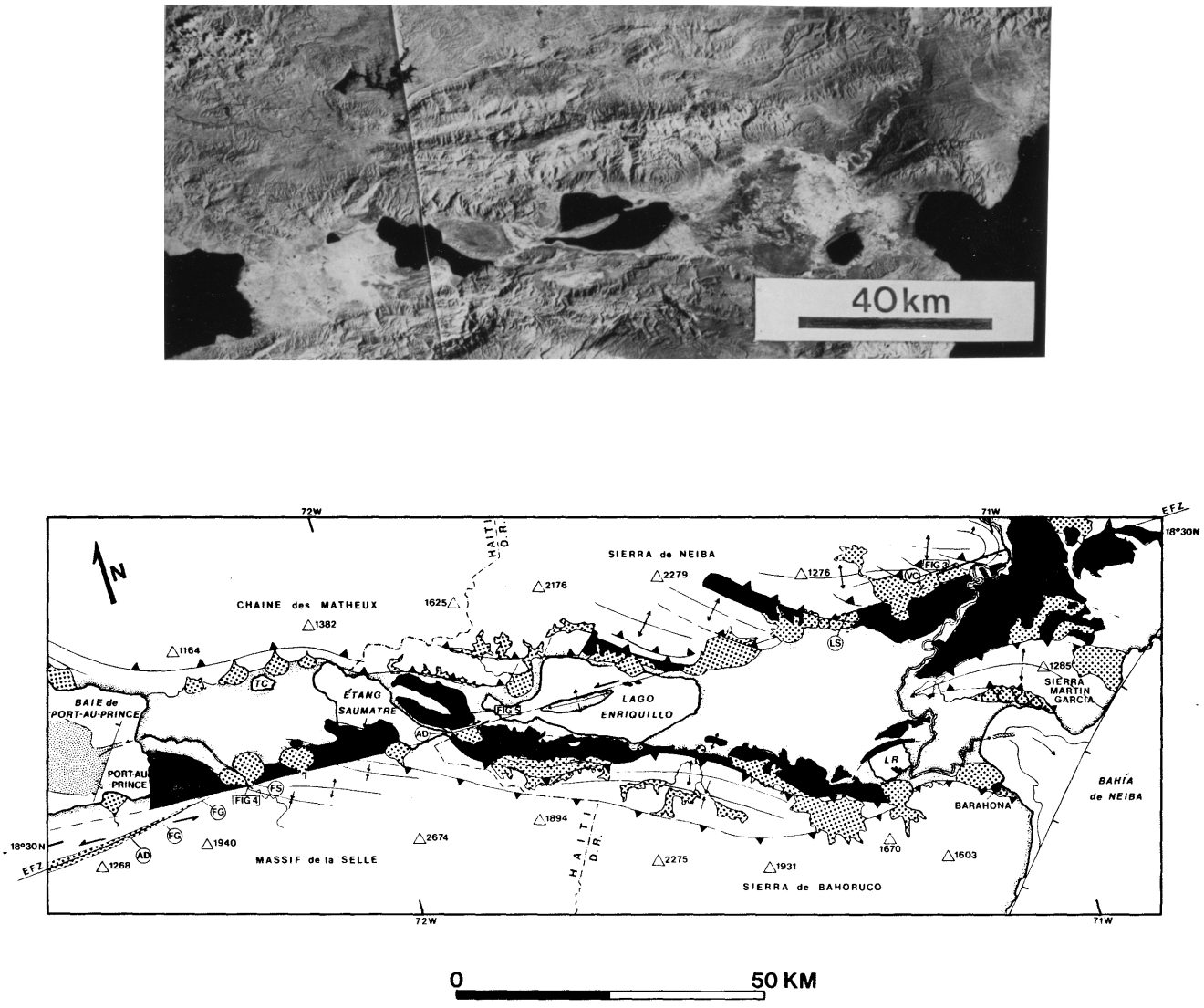

Fig 2. A. LANDSAT mosaic (2 images) showing the area of the EPGFZ in southern Hispaniola (Haiti and Dominican Republic).

B. Tectonic map of the Enriquillo – Cul-de-Sac Valley showing major structural and sedimentary features related to the EPGFZ. Dotted areas represent alluvial fans; grey areas represent the post-Miocene sedimentary rocks (mostly terrestrial); grey areas with vertical lines represent late Miocene deep marine clastic rocks deposited in a basin that was disrupted by displacements along the EPGFZ. Abbreviations for fault-related features are: 1) LS = landslide; 2) VC = vegetation contrast; 3) AD = aligned drainage; 4) FS = fault scarp; and 5) FG = fault gouge. Location of photomap of Figure 3; sketch map of Figure 4; and syncline shown in Figure 5 are indicated.

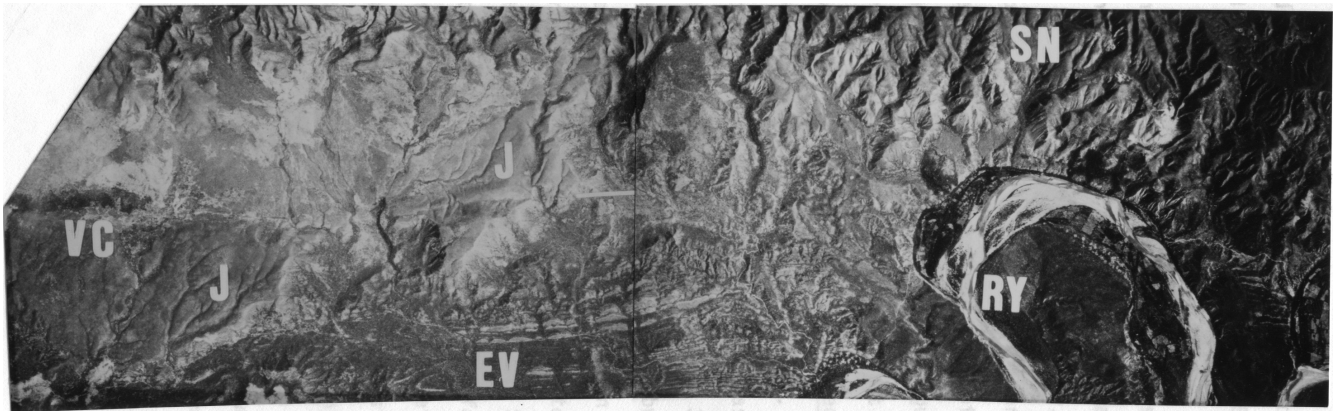

Figure 3. Fault morphological features of the EPGFZ visible on the 1:50,000 aerial photograph of the Rio Yacque del Sur area, Dominican Republic (location indicated in Figure 2 – SN = Sierra de Neiba; RY = Rio Yacque; EV = Enriquillo Valley). White line indicates trace of EPGFZ; VC = vegetation contrast; J = mesa formed by Pleistocene Jimani Limestone in which the EPGFZ scarp is well developed. Jimani Limestone north of the fault is downdropped by about 40 m and tilted northward about 10-15º (see Figure 5 for a view of this area from the east).

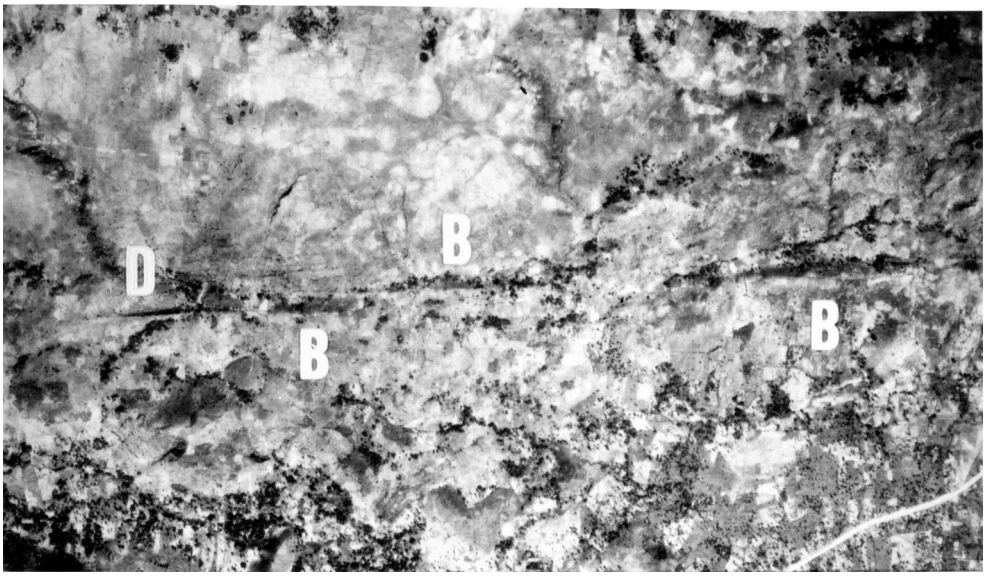

Figure 12. Fault trace of EPGFZ to the west of the Mirogoane Lakes pull-apart basin (see Figure 8B for location). B = "bulges" along fault trace; D = closed depression, possibly a small pull-apart basin.

Figure 13. View to north across northern faulted margin of the Camp Perrin Basin (see Figure 8B for location). Ridges in foreground are resistant alluvial fan deposits, deposited along a Pliocene fault scarp forming the northern edge of the basin. Hills in background are late Cretaceous limestone which supplied clasts to the fans. Valleys between fan ridges are formed by less resistant alluvial plain mudstones. Fan deposit adjacent to the basin edge contains coarser material than fan in foreground.

Figure 14. Imbricate thrust faults affecting Pliocene (?) lacustrine sandstones and shales of the Camp Perrin Basin (note 2 pens for scale).

Figure 15. Synsedimentary normal fault within Pliocene (?) lake beds of Camp Perrin Basin (note pen for scale).

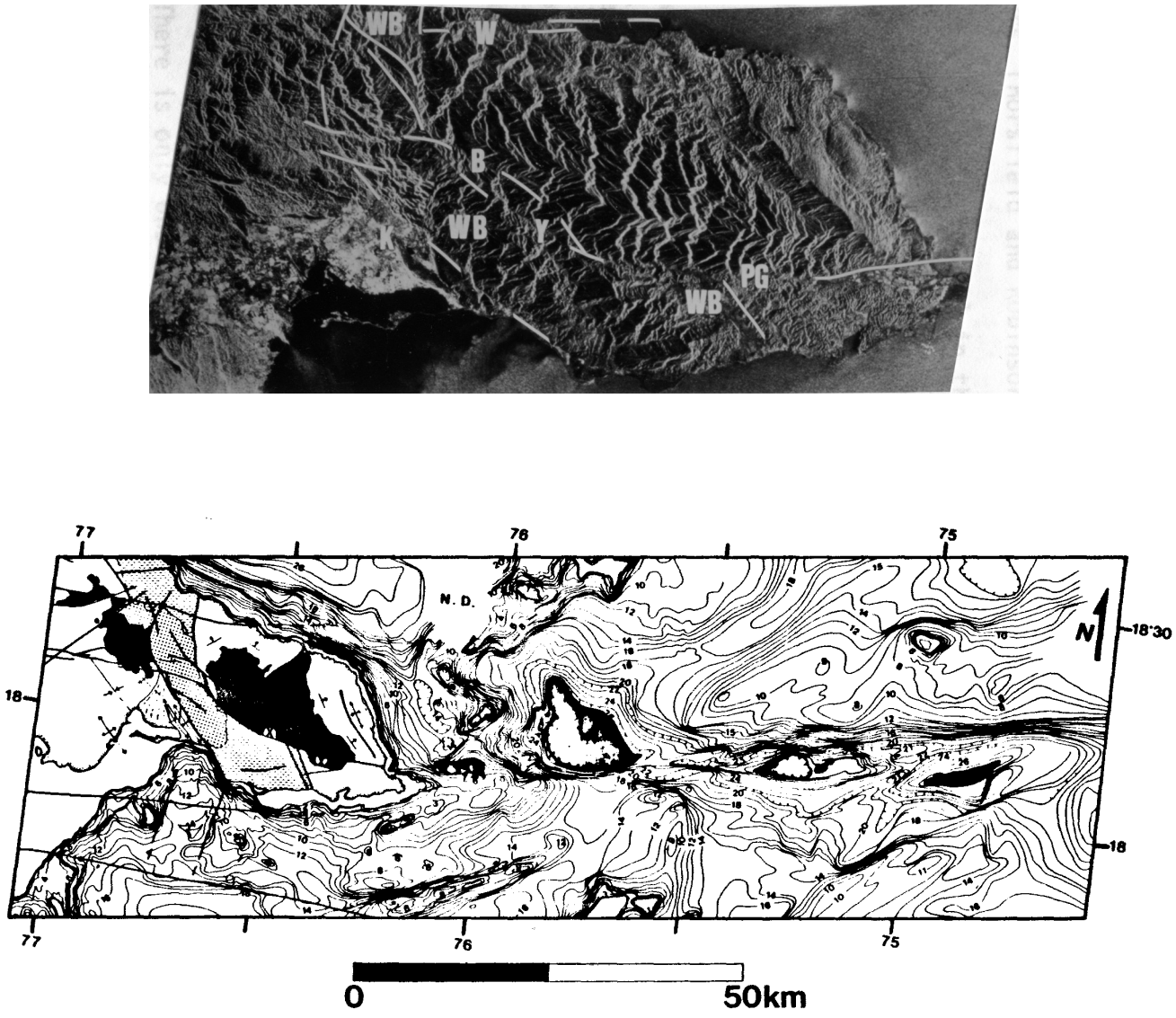

Fig 17. A. SAR radar image of eastern Jamaica (provided by T. Dixon, Jet Propulsion Lab). White lines emphasize major faults; PG = Plantain Garden Fault Zone; Y = Yallahs Fault Zone; B = Blue Mountain Fault Zone. WB indicates area of Wagwater Belt, a reactivated Paleogene graben.

B. Bathymetry of the seafloor of the Jamaica Passage (numbers represent depths in hundreds of meters) and schematic structural map of eastern Jamaica (black areas are Cretaceous arc rocks; dots represent outcrop of older Paleogene redbed fill of the Wagwater Graben exposed in an elliptical dome; horizontal lines represent outcrop of younger Eocene fill of the Wagwater Graben; “X's” indicate maximum apparent left-lateral offset of EPGFZ of about 10 km.)

Figure 19. Faceted spur along the Plantain Garden Fault Zone, southern Blue Mountains (view towards east).

Figure 21. View of the southwestern slope of the Main Ridge of the Blue Mountains. White line in middle ground is Blue Mountain Fault Zone.

Figure 22. View of the southwestern slope of the Blue Mountains from the northwest. (X = outcrop of Westphalia Schist showing apparent left-lateral offset of 3.5 km on Blue Mountain Fault Zone). Yallahs Fault Zone is to right of photo.

Figure 23. Outcrop of mylonitic limestone along the eastern edge of the Yallahs Fault Zone. Note hammer head for scale.

Figure 24. Hand sample of mylonitic limestone from the Yallahs Fault Zone.

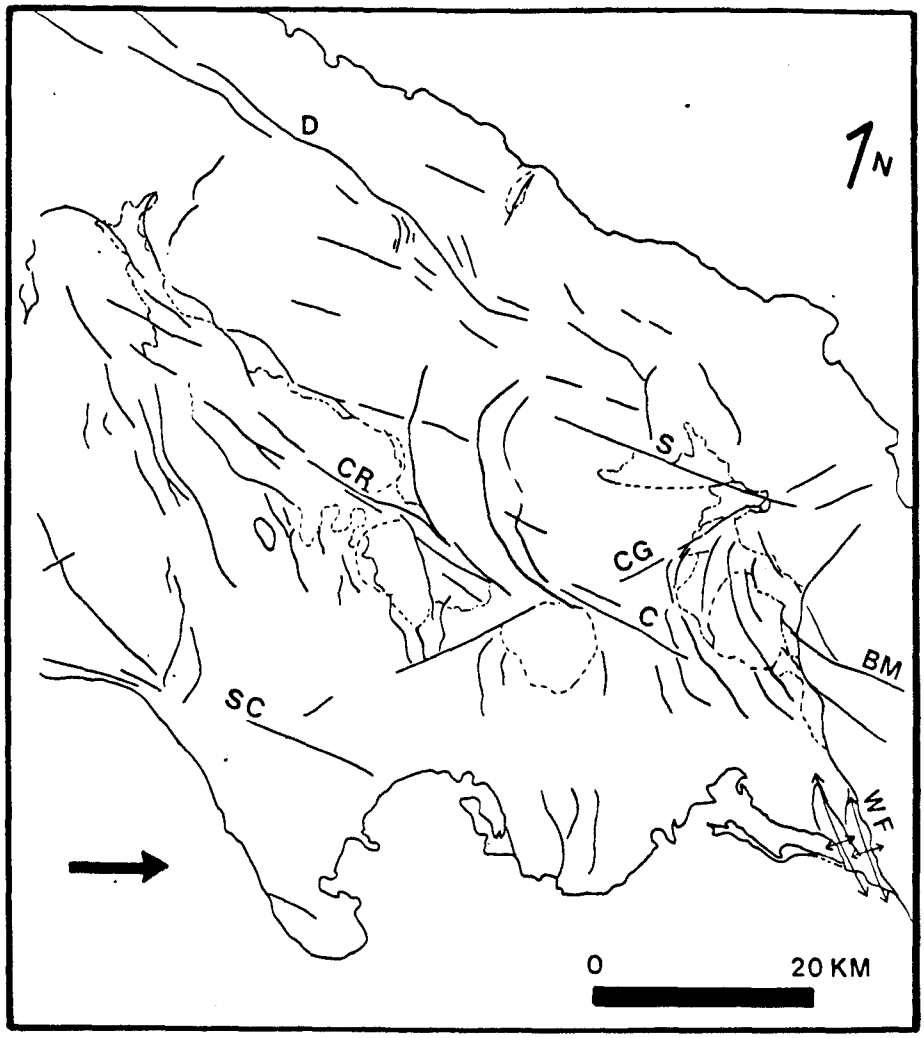

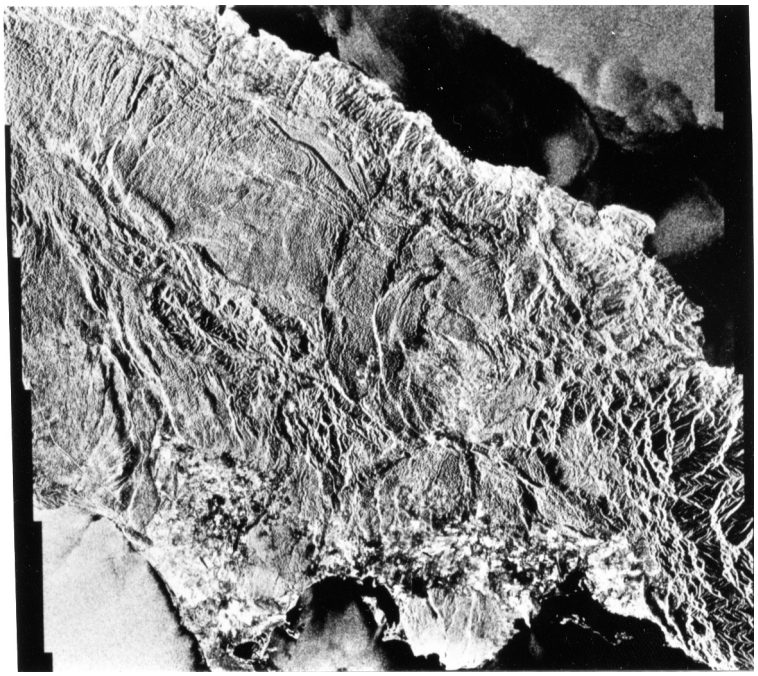

Fig 28. Radar image and fault interpretation of central Jamaica. Abbreviations are: D = Duanvale; S = Seafield; CR = Crawle River; C = Cavaliers; SC = South Coast; CG = Cuffy Gulley; BM = Blue Mountain; WF = Wagwater Fault.

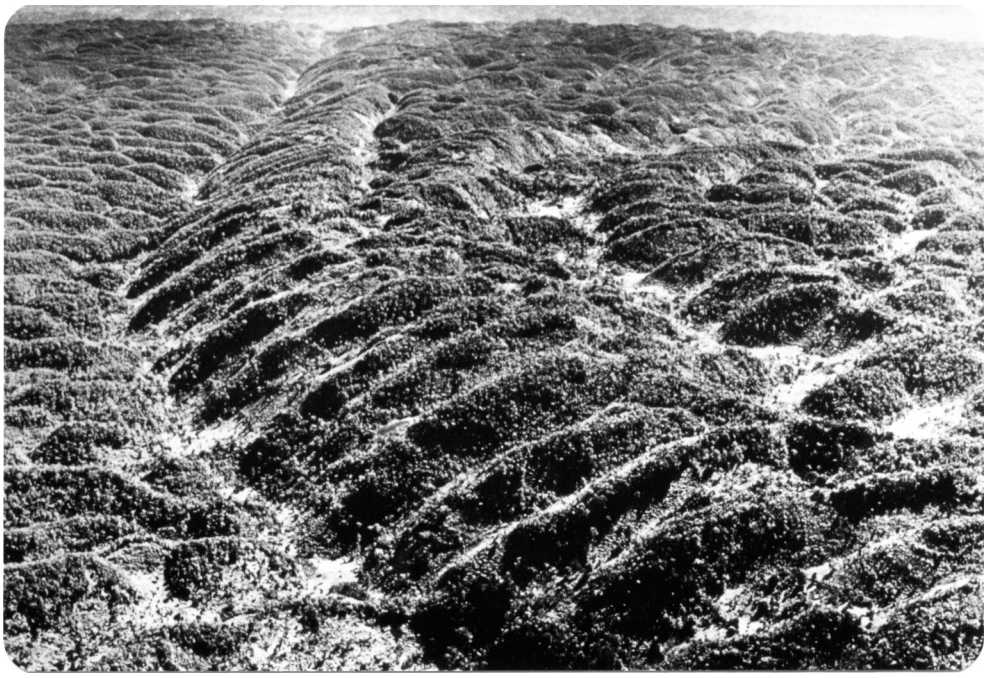

Figure 30. Aerial view looking east along the Duanvale Fault Zone (DFZ). White line in distance indicates approximate eastern termination of prominent fault trace. BM = Blue Mountains; SWF = approximate position of Seafield-Whitehall Fault Zone; PGF = approximate position of Plantain Garden Fault Zone.

Figure 5. View from the east towards mesa formed by resistant Pleistocene Jimani Limestone unit, Sierra de Neiba. Jimani limestone is downdropped about 40 m and tilted 10-15º northwards by EPGFZ. Left-lateral offsets of drainage on top of plateau (see Figure 3 for aerial view) suggest recent strike-slip displacement occurred along with vertical displacement.

Figure 6. Syncline developed in Pleistocene Jimani Limestone adjacent to EPGFZ (see Figure 2B for location).

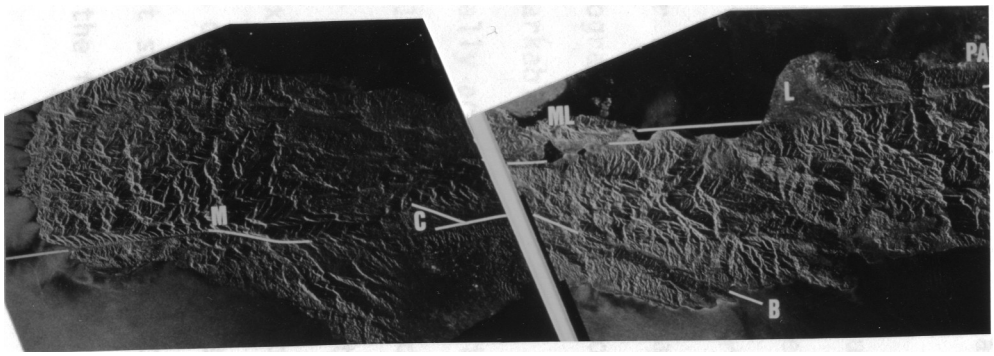

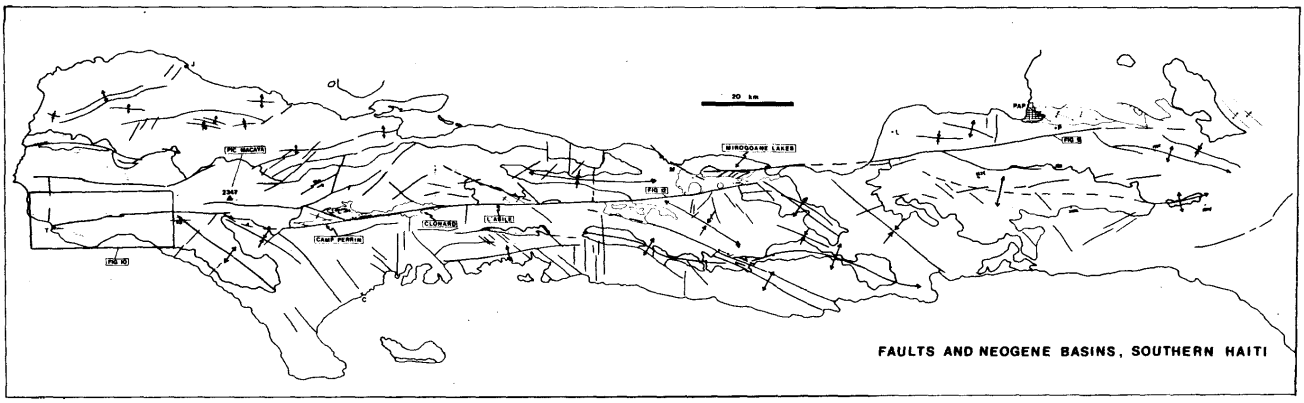

Fig 2. A. SAR imagery of southern peninsula of Haiti (provided by T. Dixon, Jet Propulsion Lab). White gap indicates missing coverage, white lines indicate trace of EPGFZ. PA = Port-au-Prince; L = Leogane; B = Bainet Fault Zone; C = Pliocene Camp Perrin fault wedge basin; M = Pic Macaya (elev. 2347 m) at Macaya restraining bend fault segment.

B. Tectonic map of the southern peninsula of Haiti modified from Duplan [1975]. Shaded areas represent Cretaceous rocks. Note Mirogoane Lakes and Clonard pull-apart basins; L'Asile and Camp Perrin fault wedge basins; and Macaya restraining bend.

Figure 9. View from the north across fault trough near Leogane (see Figure 8B for location). Fault trough is occupied by Riviere Froide. Divergent relative motion across the EPGFZ is suggested to have produced the rifting of the Paleogene limestone platform exposed on slopes at this slightly south-stepping fault segment.

Figure 4. Unconformity at location 8 (Fig. 2) separates overlying Holocene back reef deposits from Pliocene sediments, here intensely deformed along south-dipping reverse faults.

Figure 5. Outcrop of sub-columnar form of *Montastrea annularis*, between localities 4 and 5 (Fig. 2) In the absence of *Acropora palmata*, *M. annularis* provides the best indicator of the minimum elevation for paleosea level when the reef died (5 m BLS). Pen in right-center of photo is 14 cm long.

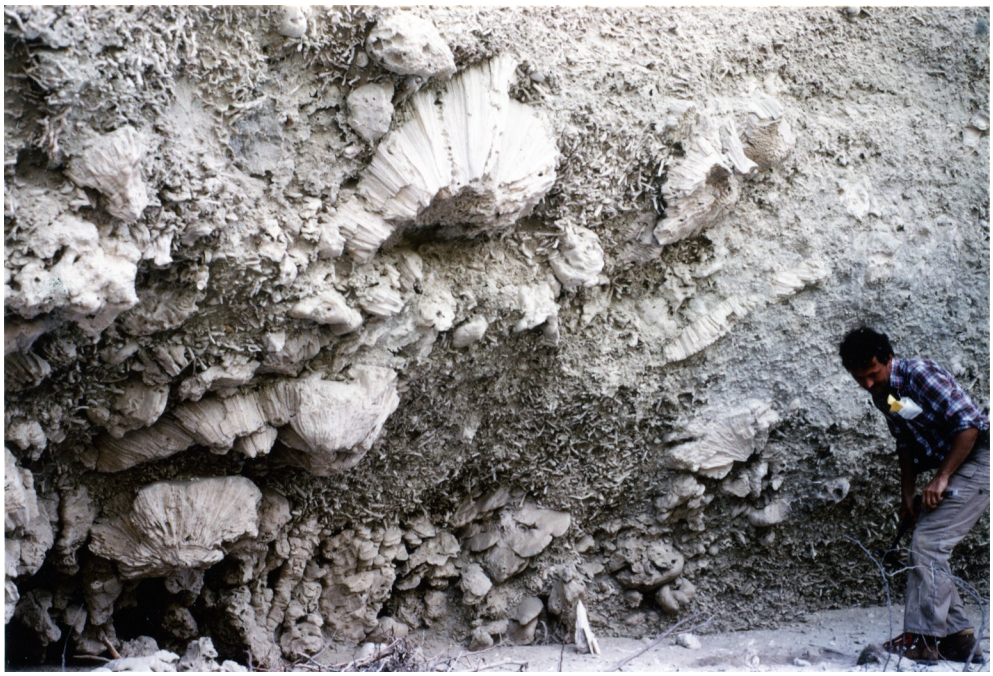

Figure 7. Main reef body, well exposed in erosional gully north of Lago Enriquillo (Fig. 3, location 1), consists of head corals enclosed within growth position and fragmented *Acropora cervicoris*. A sample collected from the center of a fresh *S. radians* head shown in this outcrop yielded a radiocarbon age of 5930 +/- 100 yr B.P. Outcrop is 60 km from the ocean. Note depositional dip of corals towards Lago Enriquillo, which lies to the left of the picture..

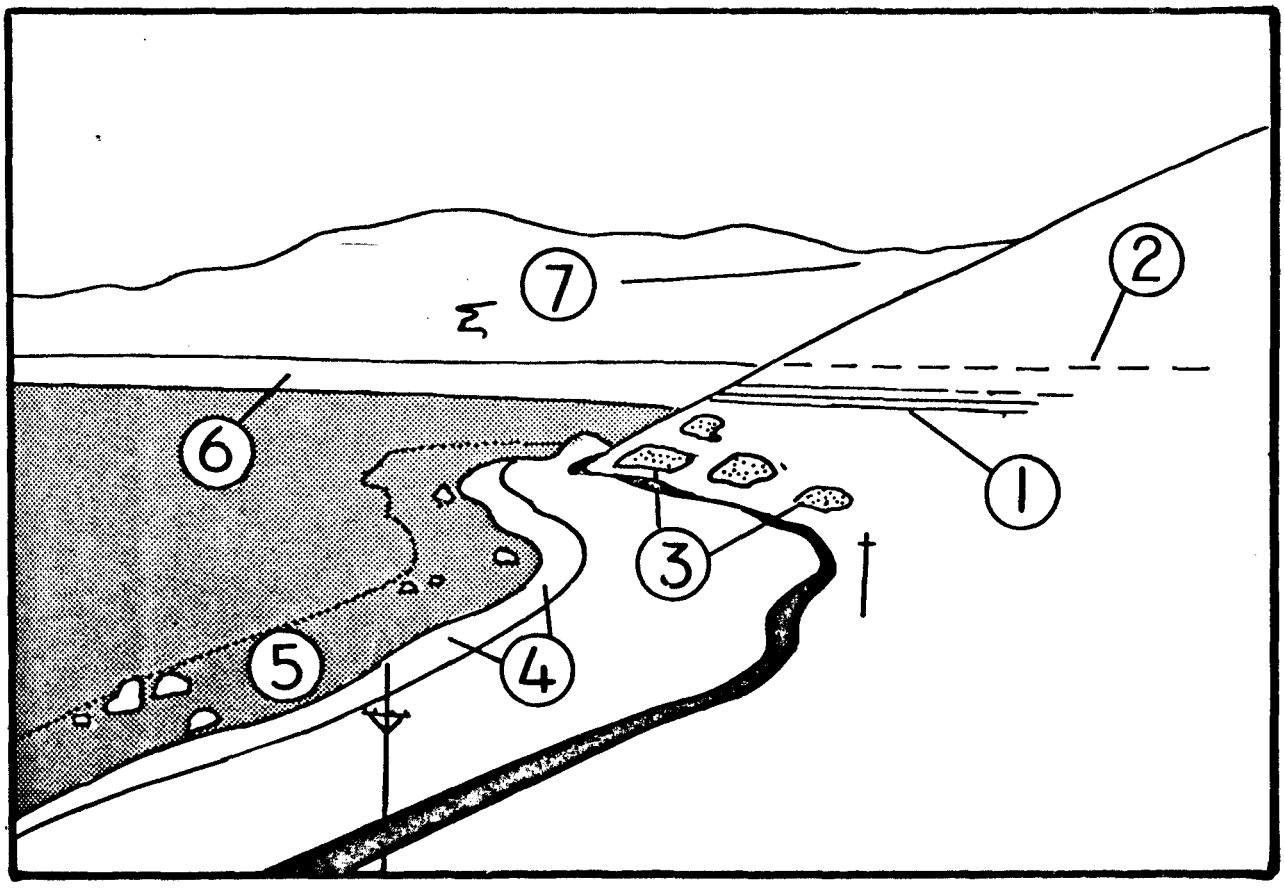

Figure 8. View of shoreline deposits from locality 5 (Fig. 3). Numbered localities are as follows: 1 = two-tiered algal tufa; 2 = upward limit of dark discoloration of limestone interpreted as a high-water mark; 3 = beachrock deposits; 4 = zone of drowned vegetation following Hurricane David in 1979; 5 = zone of partially submerged vegetation; 6 = fan-delta with overlying coral reefs; 7 = road cut.

Figure 9. Front view of well-developed shoreline algal tufa deposits, which flourished locally in the restricted marine embayment following the demise of the coral reef. This colony occurs at an elevation of 0 meters and unconformably overlies coral reef. Exposure is about 5 meters high (length of field notebook in the right-center of the photograph is 20 cm).

Figure 6. Aerial view of southwestern margin of the Wagwater Belt adjacent to Kingston. Wagwater Fault Zone is a steep reverse fault (see Section D, Figure 5) along which the Paleogene sedimentary (Wagwater and Richmond Formations) and volcanic rocks (Newcastle Volcanics) of the Wagwater Belt overthrust the alluvial plain on which the city of Kingston is built. Overthrusting has produced folding in rocks as young as Pliocene (fold axes indicated). Note the difference in topography produced by the Wagwater Belt lithologies (i.e. the Newcastle Volcanics being the most resistant to erosion and the Richmond Formation being the least resistant).

Figure 9. View of abandoned Halberstadt gypsum quarry in southeastern Wagwater Belt (near column 10 in Figure 7) where the upper contact between the Brooks Gypsum and Dry River Members of the Wagwater Formation is exposed. The white area is massive nodular gypsum; the darker area above it consists of interstitial gypsum within red mud and siltstone. This passes upsection into redbeds without gypsum. The base of the 30 m thick massive gypsum unit is a 3 m thick reefal limestone (Halberstadt Limestone). The sequence is interpreted as a supratidal (coastal sabkha) deposit formed during marine regression and is very similar to the sequence of lithologies observed in modern evaporite environments such as the Abu Dhabi Coast of the Persian Gulf.

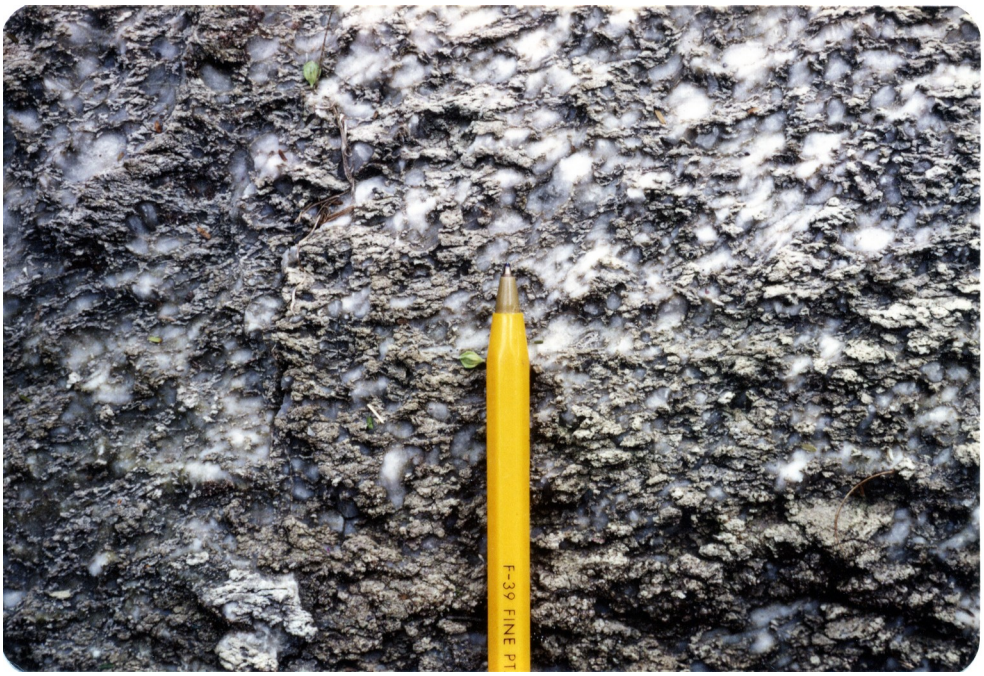

Figure 10. Interstitial gypsum within red mud and siltstone above the Brooks Gypsum Member at the Halberstadt Quarry.

Figure 11. Poorly sorted redbeds of the Dry River Member of the Wagwater Formation exposed in the seacliffs at Stileman's Cove in the northern Wagwater Belt. The conglomerates are clast-supported and pinch out into the interbedded red mud and coarse sandstone layers. The rocks are interpreted as alluvial fan deposits.

Figure 12. Clast-supported red conglomerates within a 1 meter thick bed of the Dry River Member at Stileman's Cove. Dark clasts are mainly fine grained Cretaceous volcanic rocks while lighter, speckled clasts are granodiorite. The Dry River Member is easily distinguished from the underlying members of the Wagwater Formation by the presence of granodiorite clasts.

Figure 13. Distinctive Cretaceous volcanic clast from the conglomerates of the Dry River Member exposed at Stileman's Cove. Note large 1 cm long plagioclase laths. Outcrops of a very similar type of rock occur 16 km to the south in the medial Cretaceous Devil's Racecourse Formation of the Benbow Inlier. This suggests that the Dry River Member may be composed of material eroded from the Benbow Inlier in the Paleocene.

Figure 14. Unconformity exposed at Stileman's Cove between the underlying dark red Dry River Member of the Wagwater Formation and the brown Port Maria Member of the Richmond Formation. Planar unconformity is disrupted by a normal fault that is post-depositional and probably related to Neogene strike-slip movements in the area. The similarity in the dip of both formation at this outcrop has led previous workers to the conclusion that the contact is conformable. However, regional mapping (cf. Plate IV) shows a general 20º discordance in dip across the contact. This discordance, along with the contrast in color and sedimentology, suggest that the contact is an angular unconformity.

Figure 15. Channel-shaped body of coarse sandstone within massive clast supported conglomerstes of the Port Maria Member of the Richmond Formation at the seacliffs northwest of Port Maria. The segregation of coarse sandstone into broad channels with low-angle inclined laminae suggest reworking by wave action in a coastal transitional zone. The Port Maria Member also contains conglomerates deposited in channels cutting a submarine slope. Sample shown in Figure 16 is from this outcrop.

Figure 16. Photomicrograph of coarse sandstone found at outcrop in Figure 15 (crossed polars, 3.5x). The grains are poorly sorted , calcite cemented and consist mostly of fragments of fine-grained volcanic rocks and large feldspar crystals. Calcite locally replaces parts of original grain types with plagioclase being most affected.

Figure 17. Clast-supported, massive channel fill conglomerates of the Port Maria Member west of Mahoe Bay near Port Maria. Conglomerate deposit is lens-shaped and incised into a turbiditic sandstone and shale sequence containing lens-shaped channels of a medium-coarse grained sandstone. Height of exposure is 20 m. Channel conglomerate fines upward into massive brown coarse sandstone. Note blocks of Dry River Member of the Wagwater Formation shown in Figure 18.

Figure 18. Closer view of channel fill deposit shown in Figure 17. Note blocks of poorly sorted redbeds that are very similar to the Dry River Member of the underlying Wagwater Formation (compare with Figure 11).
Note massive sandstone above coarser conglomerate deposit. Deposit is interpreted as an inner submarine channel fill sequence in which fining upwards into massive sandstone reflects progressive channel abandonment. Channel is incised in proximal submarine fan deposits. Inclusion of blocks of lithified Wagwater alluvial fan deposits indicates erosion of the Wagwater Formation probably to the southwest (direction determined from paleocurrents in overlying Roadside Member). This observation is consistent with the unconformable relationship observed between the Richmond and Wagwater Formation at Stileman's Cove (Figure 14).

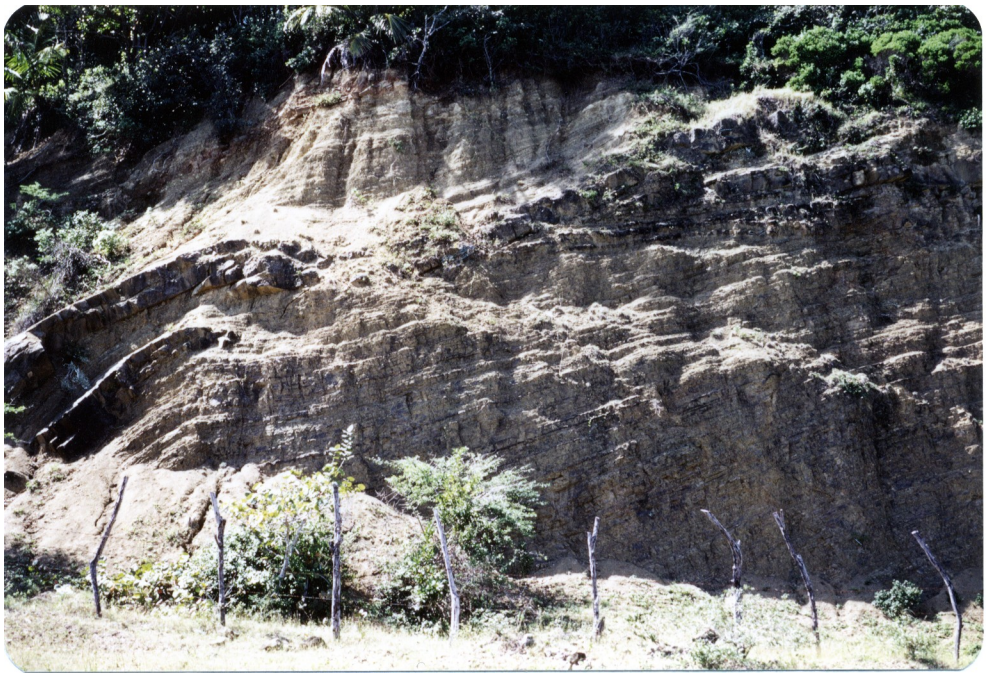

Figure 19. Channelized lenses of amalgamated sandstone beds within thinly bedded turbidites of the Roadside Member of the Richmond Formation near Port Maria. The deposit is interpreted as a channelled lobe of a submarine fan.

Figure 20. Thick turbiditic sandstone layer within the Roadside Member of the Richmond Formation near Port Maria. Sedimentary structures suggest two divisions of the Bouma model for turbidites: B is parallel laminated sandstone and C is slightly finer ripple cross-laminated sandstone. By comparison to experimental studies, B to C transition represents a decrease in the velocity of the turbidity current which deposited the grains.

Figure 21. Sand-filled burrows (probably *Thalassinoides*) within a siltstone layer within the Roadside Member near Port Maria.

Figure 22. Contact between pillow basalts of the Nutfield Volcanics and overlying thinly bedded sandstone and shale sequence of the Roadside Member at Stileman's Cove. Intermixing of basaly and sediment at the contact suggests basalt was being buried while it was still molten. The Nutfield Volcanics in the northern belt appear to be the youngest volcanics in the Wagwater Belt and are known from marine fossils in the surrounding Richmond Formation to be of early Eocene age.

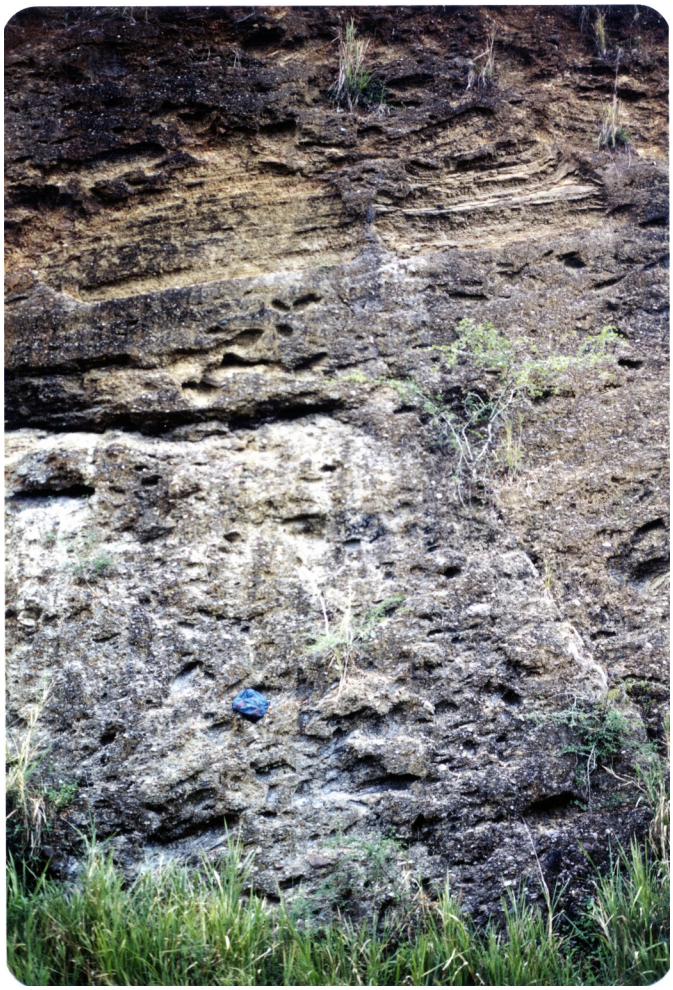

Figure 23. Massive clast supported conglomerates of the Albany Member of the Richmond Formation outcropping along the Annotto Bay-Port Maria highway between Albany and Water Valley. Blocks of thinly bedded turbidites (with deformed edges), characteristic of the underlying Roadside Member (see Figure 26) are observed in the poorly sorted deposit, which is interpreted as a submarine slope channel fill deposit. Note scour surfaces that probably represent slump surfaces.

Figure 24. Clast supported conglomerates of outcrop shown in Figure 23. The long axes of fairly well rounded clasts are parallel and indicate a debris flow origin.

Figure 25. Dominantly shale sequence within the Roadside Member outcropping along the Annotto-Port Maria highway near Albany. These deposits suggest deposition on a basin plain.

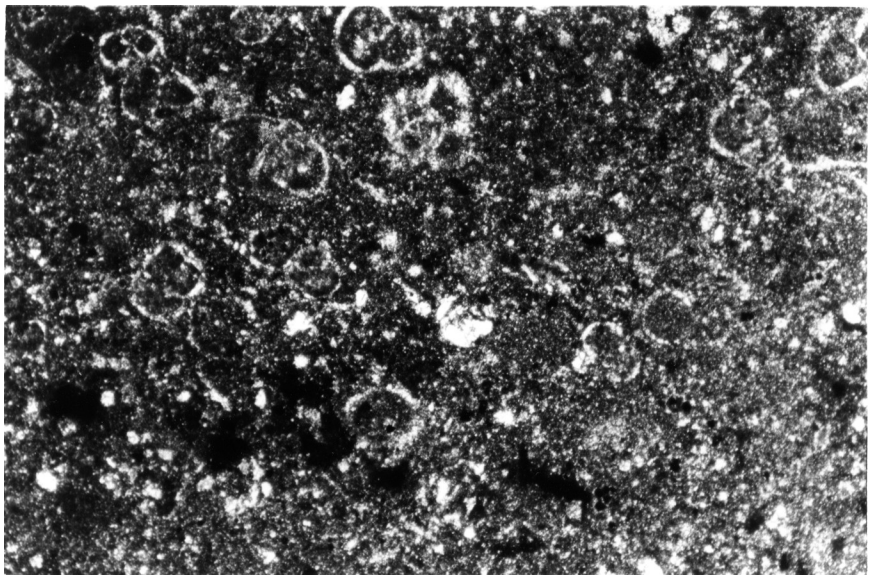

Figure 26. Photomicrograph of planktonic foraminifera (*Globogerina sp.*) within the Roadside Member (plane light 3.5x). These marine fossils indicate an early Eocene age.